SQUIDS

WILLIAM G. JENKS, IAN M. THOMAS, AND JOHN P. WIKSWO, JR., *Department of Physics, Vanderbilt University, Nashville, Tennessee, U.S.A.*

INTRODUCTION

Superconductors are best known for their ability to conduct current without developing a corresponding voltage. Perhaps a more fundamental property is the pairing of conduction electrons (see SUPERCONDUCTIVITY, LOW-TEMPERATURE). This property of the microscopic charge carriers leads to the macroscopic phenomena associated with superconductivity. It also led to the invention of the most sensitive detector of magnetic flux known, the superconducting quantum interference device, or SQUID. The SQUID is, to the engineer, a magnetic flux-to-voltage transducer of unparalleled sensitivity. It is arguably the most sensitive detector of any kind, with an equivalent energy sensitivity that approaches the quantum limit. This article should serve as a starting point to any engineer or physicist who wishes to understand SQUIDs. The principles of operation, the methods of manufacture, and the applications of SQUIDs are each discussed in turn.

1. THE PRINCIPLES OF OPERATION

1.1 The Josephson Junction

The Josephson junction (Josephson, 1962) is the heart of SQUID technology. A SQUID is in essence a superconducting loop interrupted by one (rf SQUID) or two (dc SQUID) Josephson junctions. Figure 1 shows a typical junction and the Josephson equations, which govern its electrical properties. While several physical configurations are possible, the essential feature is a thin insulating layer, or a narrow constriction, between two superconductors. The Josephson equations may be derived from Ginzburg–Landau theory (1950). The essential feature of the theory is that in any particular superconductor, an order parameter ψ exists and has associated with it an arbitrary phase θ. In two *weakly connected* superconductors, the relative phase, $\delta = \theta_1 - \theta_2$, affects the electrical properties of the junction. The dc Josephson equation relates the applied current passing through the junction to the relative phase and the critical current of the junction, I_0. Notice that if $I = 0$, then $\delta = 2\pi n$; thus a bias current must flow through the junction for a physically meaningful phase difference to exist. The ac Josephson equation relates the voltage across the junction (once $I > I_0$) to the temporal derivative of δ.

To build a SQUID, the superconductors on either side of the junction must be joined, either by a loop with a second junction (dc SQUID, shown in Fig. 2a) or by a continuous superconducting loop (rf SQUID, shown in

3-527-29300-0/97/$5.00 + .50

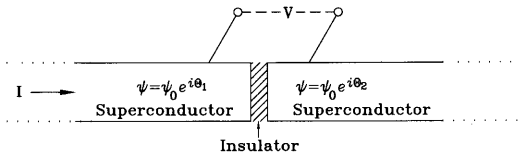

Josephson Equations

$$I = I_0 \sin\delta \quad \text{(dc)}$$

$$V = \frac{\hbar}{2e}\left(\frac{d\delta}{dt}\right) \quad \text{(ac)}$$

$$\delta = \Theta_1 - \Theta_2$$

FIG. 1. The Josephson junction and Josephson equations. A superconductor is interrupted by a thin insulating layer (cross-hatching). The phase of the superconducting order parameter ψ becomes a function of the current flow through the junction, which leads to the unique electrical properties of the junction.

Fig. 2b). A weakly connected superconducting loop is thus formed. The loop will contain flux only in multiples of the flux quantum $n\Phi_0$, where n is any integer and $\Phi_0 = 2.07 \times 10^{-15}$ Wb (see DIAMAGNETISM). Typically, the SQUID incorporates a resistor in parallel with the Josephson junction(s) to prevent hysteresis in the *I-V* characteristic. The equivalent circuit of the ideal, noise-free, resistively shunted junction (RSJ) consists of the Josephson junction, its physical capacitance, and the resistor, all joined in parallel, as shown in Fig. 2. Standard circuit analysis may be applied to the SQUID equivalent circuit, using Josephson's equations for the junction, and the resulting differential "equations of motion" can be solved numerically. This approach leads to the so-called washboard-potential model.

1.2 The dc SQUID

In the dc SQUID, a change in applied flux, Φ_A, leads to a phase difference across the junctions, giving rise to a voltage across the loop that we may detect. The characteristic *I-V* curves of the dc SQUID are shown in Fig. 3(a) for $\Phi_A = n\Phi_0$ and $\Phi_A = (n + \frac{1}{2})\Phi_0$, where n is any integer. If the bias current is held constant, the SQUID voltage will vary between two values, $V_{\min}$ and $V_{\max}$, as the flux applied to the SQUID varies between $n\Phi_0$ and $(n + \frac{1}{2})\Phi_0$. The V-Φ_A curve is thus roughly sinusoidal, as shown in Fig. 3(b), with period Φ_0. Figure 3(c) shows that a small flux modulation, $\Phi_m \sin(\omega t)$, where $\Phi_m \leq \Phi_0/2$, applied to the SQUID operating at three different points, *A*, *B*, and *C*, on the V-Φ_A curve will elicit three different voltage responses, V_s. At points *A* and *C*, V_s is at the same frequency as Φ_m, while at point *B*, where $\Phi_A = (n/2)\Phi_0$, V_s is at a frequency of 2ω. Thus the SQUID acts as a nonlinear flux-to-voltage transducer.

To linearize the V-Φ_A curve, we introduce the flux-locked loop (FLL) in Fig. 4. The FLL maintains lock by keeping the system at $\Phi = (n/2)\Phi_0$, one of the extrema in the V-Φ curve. A modulating flux $\Phi_m(\omega)$, where $\Phi_m \leq \Phi_0/2$, is applied to the SQUID, at frequency ω, by the oscillator. The response of the SQUID is fed into a lock-in amplifier, referenced to the oscillator. If the dc flux in the SQUID is a multiple of $(n/2)\Phi_0$, then the output of the SQUID is a periodic function of 2ω and the lock-in amplifier will put out 0 V dc. If the dc flux strays from an extremum by $\Delta\Phi$, then the SQUID output will contain a component at ω and the lock-in will put out a dc voltage, V_L, proportional to the amplitude of the signal at ω, as shown in the third line of Fig. 3(c). This dc signal is essentially an error signal; it is integrated and fed back into the modulation coil as $-\Delta\Phi$, returning the SQUID flux to $(n/2)\Phi_0$. The output of the loop, V_0, is a voltage proportional to the feedback current, controlled by V_L (which is proportional to $\Delta\Phi$.) The user records V_0 and relates that to the magnetic field through a prior calibration with a known field. The reader should note that many FLL oscillators put out a square-wave flux modulation with amplitude $\Phi_0/4$ and frequency ω. The system then shifts between $\Phi = (n/2 + \frac{1}{4})\Phi_0$ and $\Phi = (n/2 - \frac{1}{4})\Phi_0$, still centered on an extre-

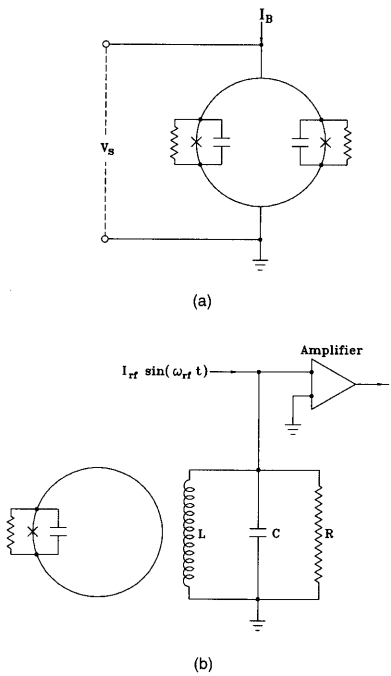

FIG. 2. (a) Schematic of a dc SQUID loop. The superconducting loop is interrupted by two Josephson junctions, marked by x. The dc SQUID is biased with a dc current. (b) Schematic of an rf SQUID loop. The rf SQUID has one Josephson junction. The rf SQUID is coupled to an rf tank circuit. The Josephson junctions are each shunted by a resistor. The physical capacitance of the junction is shown as well, because it must be considered in an accurate model of the electrical properties of the SQUID.

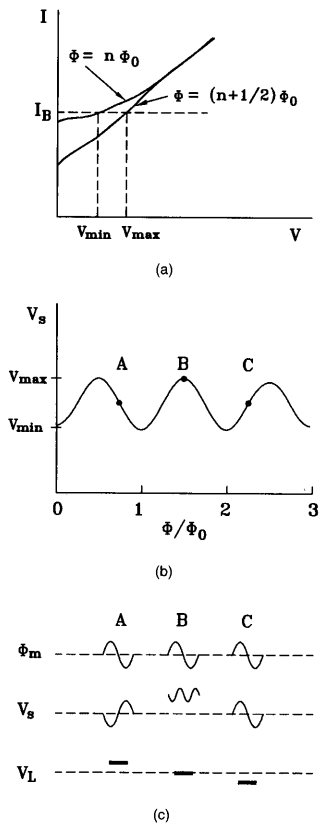

FIG. 3. (a) The *I-V* characteristics of a dc SQUID. The amount of applied flux, Φ_A, determines the voltage output V_s for a particular value of bias current I_B. As the applied flux varies between $\Phi_A = n\Phi_0$ and $\Phi_A = (n + 1/2)\Phi_0$, the output voltage changes between V_{min} and V_{max}. (Adapted from Clarke, 1989.) (b) The V-Φ curve of a dc SQUID, with constant bias current. (c) The voltage response of the SQUID to a modulating flux, Φ_m. The response varies greatly depending on the value of Φ_A. Three possible points are highlighted to illustrate the response of a SQUID and the feedback needed to "lock" the SQUID to operation at an extreme value. From top to bottom we see one cycle of the flux modulation, Φ_m, applied to the SQUID operating at three different locations on the V-Φ curve; the voltage response of the SQUID, V_s; and the necessary feedback of the flux-locked loop, V_L, which applies a counter flux to the SQUID loop (see text), returning the system to an extreme position on the V-Φ_A curve.

mum but spending very little time at the extremum.

The flux-locked SQUID has a bandwidth that is some fraction of the modulation frequency, typically 100-kHz modulation and 10-kHz bandwidth. If the applied flux changes too rapidly for the feedback electronics to track, then the SQUID jumps from one extremum to another, and the SQUID is said to have lost lock. The maximum change in flux per unit time that the system can tolerate while maintaining lock is the slew rate, typically $\approx 10^6 \Phi_0$/s.

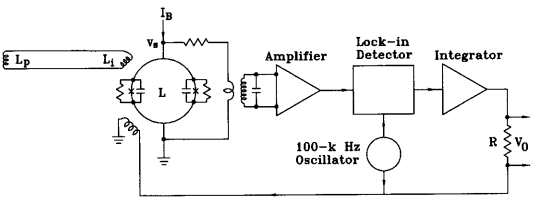

FIG. 4. Schematic of the pickup coil, input coil, SQUID and flux-locked loop (adapted from Clarke, 1989). A change in magnetic field at the pickup coil, with inductance L_p, induces a change in field at the input coil, with inductance L_i; the SQUID is inductively coupled to the input coil, and it detects a change in magnetic flux. The voltage response of the SQUID, V_s, is then fed into the flux-locked loop. The loop uses a modulating flux scheme, explained in the text, to maintain the SQUID at an extremum on the V-Φ curve. The user measures a change in V_0, which is proportional to the feedback from the loop and to the change in magnetic field at the pickup coil.

1.3 The rf SQUID

Conceptually, the operation of the rf SQUID is very similar to that of its dc counterpart. The rf SQUID is inductively coupled to a tank circuit, as shown in Fig. 2b, being driven at a frequency $f_{rf} \approx 20$–30 MHz. If the magnitude of the radio-frequency current in the tank circuit, I_{rf}, is kept constant, then the voltage across the circuit, V_{rf}, will be periodic with any flux applied to the SQUID. This holds true because of the hysteretic nature of flux in the SQUID loop. The V_{rf}-Φ curve is then linearized with a FLL in a manner similar to the dc SQUID. In this case, the modulating flux is applied through the inductor in the tank circuit.

1.4 The Pickup Coil

The SQUID is an excellent sensor of magnetic flux. To enhance its capabilities, most SQUID systems do not expose the bare SQUID to the magnetic field of interest; rather they typically employ a multiple-turn pickup coil inductively linked to the SQUID, as shown in Fig. 4. The pickup coil, with inductance L_p, is exposed to the environment, while the input coil, with inductance L_i, and the SQUID, with inductance L, are shielded from the ambient field by a superconducting niobium canister. Typical values for the inductances are $L_p = L_i = 1$ μH and $L = 0.1$ nH. Historically, all pickup coils were hand wound of superconducting wire, but in some thin-film configurations, the pickup coils are fabricated on the same chip as the SQUID or an adjacent "flip chip" using integrated circuit technology.

1.5 Noise in the SQUID

SQUID noise is quoted in different units by different members of the SQUID community. The given noise figure is generally a power spectral density in terms of energy (J/Hz), magnetic flux (Φ_0/Hz$^{1/2}$), field (fT/Hz$^{1/2}$) or field gradient [fT/(cm Hz$^{1/2}$)]. The distinction is important as one system (of special design) can have poor field sensitivity, despite superior energy sensitivity in the SQUIDs it contains. The energy and flux noise are figures of merit (FOM) for the bare SQUID, while the field and field-gradient noise are FOMs for the complete SQUID system. As a rule of thumb, the SQUID researcher quotes energy or flux noise, while the SQUID system builder begins with the flux figure and designs for the best possible field or field-gradient noise, which is of paramount interest to the end user. Typical orders of magnitude for commercial dc SQUIDs are noise energy $\epsilon = 10^{-31}$ J/Hz; magnetic flux noise $S_\Phi^{1/2} \sim 10^{-6}$ Φ_0/Hz$^{1/2}$; and magnetic field noise $B_N = 10$ fT/Hz$^{1/2}$.

Approximate formulas for the dc SQUID noise parameters are

$$S_\Phi = \frac{(4k_B T R_D^2/R)[1 + \frac{1}{2}(I_0/I)^2]}{(R/L)^2}, \qquad (1)$$

$$\epsilon = \frac{S_\Phi}{2L}, \quad B_N = \frac{L_p + L_i}{\alpha\sqrt{L_i L}} \frac{S_\Phi^{1/2}}{A_e}, \tag{2}$$

where R_D is the dynamical resistance ($\partial V/\partial I$) of the junctions, A_e is the effective area of the pickup coil, and α is the coupling coefficient between the input coil and the SQUID. In discussing SQUID systems, the coupled energy sensitivity, ϵ/α^2, is often quoted rather than ϵ.

In the case of the rf SQUID, things are a bit more complex. The flux noise spectral density is given by

$$S_\Phi \approx \frac{(LI_0)^2}{\omega_{rf}} \left(\frac{2\pi k_B T}{I_0 \Phi_0}\right)^{4/3}, \tag{3}$$

and the energy and field resolution have additional terms due to the room-temperature electronics.

Flicker or $1/f$ noise does exist in thin-film SQUIDs, but only below ~0.1 Hz does it begin to dominate in conventional niobium SQUIDs. At the current time, low-T_c dc SQUIDs are considerably less noisy than rf SQUIDS, except for rf SQUIDs operating at microwave frequencies. Thus most end users who need superior field resolution utilize dc SQUIDs. The rf SQUIDs dominated the market prior to the introduction of thin-film dc SQUIDs in the late 1970s; rf SQUIDs still command a substantial market share today.

1.6 The Digital SQUID

Digital SQUIDs attempt to replace the conventional room-temperature analog electronics of the FLL with either a room-temperature digital signal processor (DSP) or an on-chip (4.2 K) integrated Josephson-junction feedback circuit that involves flux counting. The DSP circuits are being used successfully by a growing number of research groups; the integrated digital SQUID is promising, but the technology is still immature and underperforms conventional systems. However, the interest in further development is spurred by the increasing number of channels being used in neuromagnetism. On-chip feedback would eliminate a great deal of the cost of electronics in systems of 100+ SQUIDs and allow for simpler cryogenic design as well, particularly by drastically reducing the number of wires between room temperature and the SQUIDs.

2. DESIGN AND MANUFACTURE OF SQUIDS

A single SQUID is not a particularly difficult item to manufacture. Consistently producing low-noise SQUIDs that integrate ideally into instrumentation is the technical challenge. Here we discuss the early SQUIDs, the modern thin-film SQUIDs, high-T_c SQUIDs, and the design considerations for manufacture.

2.1 Conventional SQUIDs

Some of the earliest SQUIDs were machined from blocks of niobium. Figure 5 shows two of these designs. Figure 5(a) depicts the simple "point-contact" dc SQUID (adapted from Zimmerman and Silver, 1966). The sharpened niobium screws could be adjusted, once the SQUID was immersed in liquid helium, until the proper *I-V* characteristic was obtained. Simple designs like this achieved flux resolution of $\sim 10^{-3}\Phi_0/\mathrm{Hz}^{1/2}$ in the late 1960s. Figure 5(b) shows a cross section of the very useful "toroidal" rf SQUID (Goodman *et al.*, 1973; Rifkin and Deaver, 1976). The smaller toroidal cavity contained the tank circuit, and the larger cavity contained the input coil, which is connected to the pickup coil. This self-screening design was a commercial success, and extensive work was done with this SQUID in biomagnetism during the late 1970s and early 1980s. The flux resolution was at least an order of magnitude better than contemporary dc SQUIDs, and the SQUID noise was white between 1 Hz and several kHz.

The modern thin-film SQUIDs are typically manufactured by sputtering of niobium thin films and patterning the films with photolithography or electron-beam lithography (see SPUTTERING; THIN-FILM DEPOSITION). In principle, any superconducting material can be used to manufacture SQUIDs, but in practice, niobium technology completely dominates the low-T_c commercial SQUID market. The junction itself may be a Nb/NbO_x/Pb or Nb/Al_2O_3/Nb trilayer, while the resistive shunts can be a thin film of copper, gold, or nearly any metal that does not be-

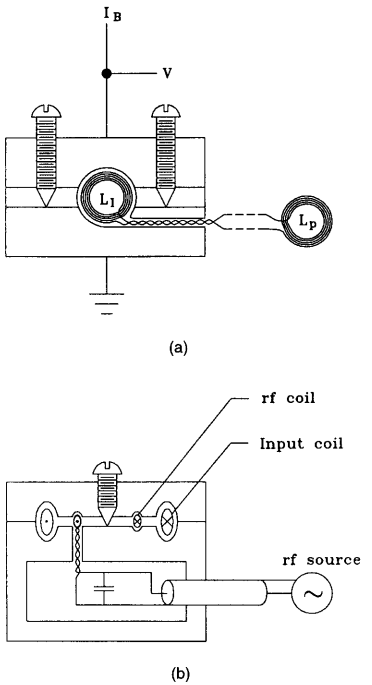

FIG. 5. Early SQUID designs machined from niobium. The Josephson junctions were made by adjusting the screws in liquid helium until the expected behavior was achieved. (a) The dc SQUID. The input coil, with inductance L_i, is linked to the pickup coil located near the magnetic sample. (b) The rf "toroidal" SQUID. The inner toroidal cavity contains the coil for the rf circuit, while a separate chamber houses the capacitor and the outer cavity holds L_i.

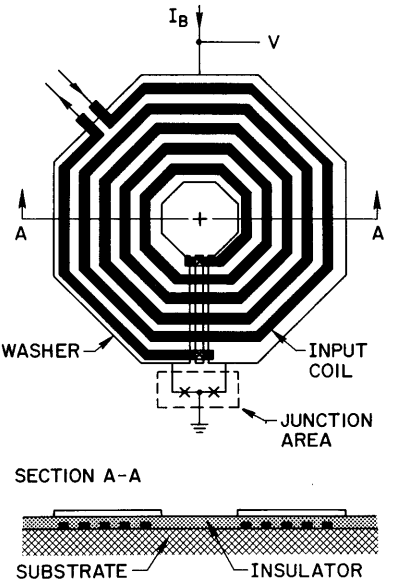

FIG. 6. A schematic drawing of a washer-type dc SQUID. The design has a very high mutual inductance between the input coil and the SQUID loop. The input coil, marked in black, is manufactured with the SQUID loop, which consists of the octagonal washer and the Josephson junctions, each marked by an x. Note that the washer is not a complete octagon; it is interrupted in two places, and the resulting bridge is used to complete the input coil. A cross section through the SQUID is shown at the bottom of the figure. The pickup coil, not shown, is connected to the input coil by the two leads in the upper left. In niobium, low-T_c technology, the entire structure is less than 1 mm across, while the junctions can be as small as 5 μm wide; the hole in the washer is typically 50–100 μm in diameter. (Courtesy of Mark Ketchen of IBM T.J. Watson Research Center.)

come superconducting at 4 K. Figure 6 shows an advanced design of the washer-type dc SQUID developed at IBM (Jaycox and Ketchen, 1981). This geometry provides SQUID loops with low inductance and hence high sensitivity, while allowing efficient coupling to an external flux transformer. Other dc SQUID designs have also been implemented for commercial SQUIDs.

The two characteristic physical parameters of a SQUID most often quoted in the literature are the reduced inductance β and the hysteresis parameter β_c, sometimes referred to as the Stewart–McCumber parameter:

$$\beta = \frac{2I_0L}{\Phi_0}, \quad \beta_c = \frac{2\pi I_0R^2C}{\Phi_0}, \tag{4}$$

where R and C are the resistance and capacitance of the resistively shunted Josephson junction and L is the inductance of the SQUID loop. These parameters emerge quite naturally in an analysis of the differential

"equations of motion" that govern operation of the dc SQUID. We see that these parameters are dimensionless, and that β is a function of the physical dimensions of the loop and the critical current of the junction, while β_c is a function of the resistively shunted junction alone. Numerical simulations of SQUIDs with various parameters have shown that for minimum noise energy β should approach unity. To avoid hysteresis β_c should be at or below 1. These conditions still give the manufacturer quite a bit of freedom, which may be used to design the SQUIDs for optimum *system* performance. To optimize the system performance, the manufacturer must achieve the highest possible signal-to-noise ratio for the signal of interest to the user in the environment of the user facility. Therefore, the system must be designed with foreknowledge of the signal of interest and the operating environment. The SQUID should be designed to couple as well as possible with the input coil, which should be impedance matched with the desired pickup coil (see below). The pickup coil must be designed to reject noise fields and to couple efficiently to the signal of interest. The designed SQUID noise should at all times be less than that of the amplifier used in the flux-locked loop. There is no single prescription for optimum performance, and SQUID design is still something of an art.

2.2 High-T_c SQUIDs

High-temperature superconductivity holds one great promise for SQUID builders and users: It will make the construction and operation of SQUID systems cheaper. The niobium SQUIDs described so far generally operate at liquid-helium temperature (4.2 K); the high-T_c systems being designed today operate at liquid-nitrogen temperature (77 K). The lower cost and greater cooling capacity of liquid nitrogen saves roughly a factor of 10^3 in the operating cost for systems in metropolitan areas and far more for remote systems. Construction costs will also be reduced as liquid-nitrogen systems are simpler and easier to build (see CRYOGENICS). The ultimate high-T_c SQUID performance will probably be inferior to the low-T_c counterpart. This is evident from the equations above for flux noise, since in dc and rf SQUIDs the flux noise scales with the temperature, i.e., by a factor of ~20.

Thin-film SQUIDs have been constructed from all the main families of high-T_c compounds: Y-Ba-Cu-O, Bi-Sr-Ca-Cu-O, and Tl-Ba-Ca-Cu-O. The material that has come to dominance is $YBa_2Cu_3O_{7-x}$. Josephson junctions have been manufactured in a number of ways using this material. The two main types of junction are grain-boundary and superconducting-normal-superconducting (SNS) junctions, i.e., $YBa_2Cu_3O_{7-x}$-N-$YBa_2Cu_3O_{7-x}$ junctions, where N represents a normal metal such as gold or silver. At the current state of the technology, the best grain-boundary SQUIDs have the lowest noise, but the best SNS junction SQUIDs are more rugged, reproducible, and manufacturable. The main difficulties with virtually all high-T_c SQUIDs fabricated to date are high $1/f$ noise below 1 Hz and poor performance when operated in weak environmental magnetic fields such as that of the Earth. The high $1/f$ noise precludes many applications in medicine and biophysics where the signals of interest have component frequencies as low as 0.05–1 Hz. Extreme sensitivity to environmental noise is a serious problem in the development of high-T_c SQUID systems, primarily because high-T_c magnetic shields and wire do not perform as well as the equivalent niobium components. This is likely to be a problem for some time, as all known high-T_c compounds are extreme type-II superconductors, which lose perfect diamagnetism at very low critical fields, H_{c1}. Electronic synthetic gradiometer systems, which incorporate multiple SQUIDs, are now being developed to allow high-T_c systems to function in noisy environments (Koch *et al.*, 1993). However, high-T_c SQUIDs already demonstrate lower noise than fluxgate magnetometers and may soon see commercial application in geophysics and nondestructive testing. The best high-T_c SQUIDs are getting better, and the optimum high-T_c SQUID is still to be made.

3. SQUID SYSTEMS

The vast majority of SQUID applications are concerned with the measurement of a magnetic field, in which the phenomenon of interest (usually a current, magnetization, or magnetic susceptibility distribution) gener-

ates a magnetic field or distorts an applied magnetic field. SQUID magnetometers, gradiometers, and susceptometers can be readily optimized for specific measurements. A typical SQUID instrument is depicted in Fig. 7. We see that the SQUIDs are located inside a small magnetic shield (e.g., superconducting niobium). Superconducting pickup coils are located at the bottom of the Dewar; the SQUID electronics are at room temperature, but close to the Dewar; and the magnetic object is placed beneath the instrument. If the experiment is conducted in an applied magnetic field, then the instrument is a susceptometer.

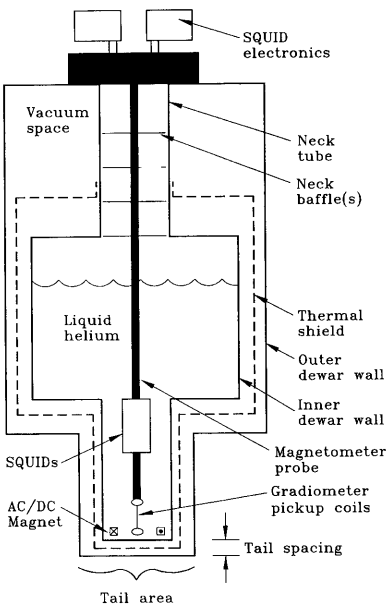

FIG. 7. A cross-sectional schematic of a simple low-T_c SQUID system. The SQUID and input coil are housed in a superconducting niobium cylinder; they are inductively coupled to an axial gradiometer near the tail of the Dewar. The flux-locked loop is housed in the SQUID electronics box above the Dewar and linked to the SQUID through the magnetometer probe. The Dewar is filled with liquid helium (boiling point 4.2 K) to cool the superconducting SQUID, niobium canister, and pickup coils. The Dewar is insulated by a vacuum space between the inner and outer walls. The instrument may be used to sense the intrinsic magnetic field of a sample or, with the magnet energized, it can measure the response of the sample to an ac or a dc magnetic field. (Adapted from Fagaly, 1990.)

3.1 Gradiometers

Although a simple single- or multiple-loop pickup coil (a magnetometer coil) can be used to measure one component of the magnetic field, such as B_z, there are a number of disadvantages to this approach, the most important of which are the contamination of the signal by environmental noise and extreme sensitivity to tilt in the Earth's magnetic field. Since the field of interest is generally orders of magnitude smaller than power-line noise, fields from passing vehicles, and radio-frequency interference, some means of background field rejection is required. This can be done either by shielding the entire experiment (as described in the next subsection), or with gradiometry. Gradiometers take advantage of the mathematical form of the falloff of magnetic fields with distance from the source. The local source of interest generates a much larger field gradient at the detector than does the more distant noise source, even though the absolute noise field is larger. Thus, by configuring coils to sense the magnetic field at two or more locations, it is possible to discriminate against the distant sources and in favor of the local one. The input coil is linked in series with two or more pickup coils, which are outside the SQUID's niobium shield. For example, we may sense $B_z(z_1)$ with one loop of the gradiometer coil and $B_z(z_2)$ with a second loop wound in the opposite sense, and the SQUID reports a voltage proportional to $\Delta B_z/\Delta z$. Commercial magnetometers are generally supplied with a hermetically sealed, shielded SQUID and two input terminals so that custom-designed gradiometers appropriate to the particular experiment and magnetic environment can be connected (see Fig. 8) (Wikswo, 1978).

3.2 Shielded Rooms

In hostile environments (such as hospitals and research facilities), the noise rejection achieved by a gradiometer may be insufficient. In these cases, the most reliable

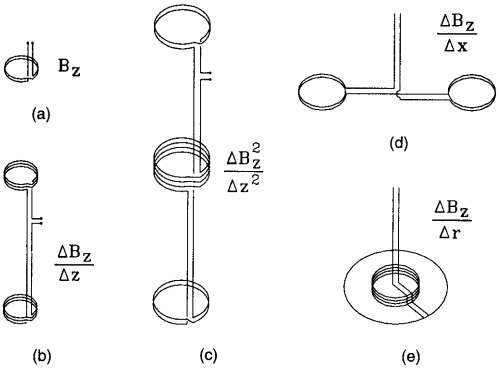

FIG. 8. A variety of pickup coil designs and the physical quantity they measure. (a) Magnetometer. (b) First-order axial gradiometer. (c) Second-order axial gradiometer. (d) First-order planar gradiometer. (e) First-order radial gradiometer.

(though expensive) solution is to carry out measurements inside a magnetically shielded room. A closed shell (access ports can be designed that do not significantly compromise the shielding) consisting of welded aluminum plates can provide eddy-current shielding of about 100 dB above 1 Hz. At low frequencies, however, structures made from high-permeability, soft ferromagnetic materials such as Mumetal or Permalloy are required. Many practical shielded rooms employ both methods.

3.3 Cryogenic Dewar Design

Liquid helium is required to maintain conventional (low-T_c) SQUIDs and input circuits in the superconducting state. Although some continuous-flow cryostats have been used, the superconducting components are generally immersed in a helium reservoir, which is thermally insulated with a vacuum jacket containing carefully designed radiation shields. The expense of liquid helium makes the boiloff rate an important consideration. Dewars are constructed with fiberglass-reinforced epoxy, which has been found to have suitable structural and thermal properties without introducing Johnson noise, distorting uniform noise fields, or screening the magnetometer from low-frequency signals. Most magnetometer measurements can be improved by minimizing the separation between the pickup coils and the room-temperature environment, and this has led to Dewars in which the superconducting components are in the vacuum space, thermally coupled to the helium. For neuromagnetic measurements, helmet-shaped Dewars containing large numbers of SQUID channels are used, while tubular Dewars, which allow a sample to be passed through the plane of the pickup coil, are popular for low-temperature and geomagnetic research.

Dewar design (see CRYOGENICS) is critical to recently developed SQUID imaging systems (Wikswo *et al.*, 1990). These high-resolution SQUID systems are designed to measure the magnetic field very close to the surface of quasi-two-dimensional objects. The resolution of the images is determined by the size of the pickup coil and its distance from the magnetic source: For high-resolution SQUIDs, magnetic sources in living tissue that are separated by as little as a millimeter can be discriminated. Some SQUID imaging systems are designed for samples, notably superconducting thin films or integrated circuits, that can be located within the cryogenic space, so that resolution of 10 μm or better is possible.

4. APPLICATIONS

4.1 Magnetoencephalography

The human brain, consisting of some 10^9 electrically active neurons, has been at the focus of biomagnetism research ever since it

became apparent that SQUID magnetometers had sufficient sensitivity to measure the tiny neuromagnetic fields (10–100 fT). The measurement, named magnetoencephalography (MEG), supplies information about the same physical process as its counterpart, the electroencephalogram (EEG). The widely cited advantage of MEG is that the magnetic field generated by cortical neurons is not distorted by the intervening bone and tissue, as are the electrical voltages recorded by the scalp EEG. The primary disadvantage is the capital and operational cost of the MEG instrumentation. Most researchers agree that a complementary approach, using both the MEG and EEG, is optimum. One of the earliest clinical MEG applications was to epilepsy. It was shown by Modena *et al.* (1982) and Barth *et al.* (1982) that interictal spikes, occurring between seizures, could sometimes be detected magnetically but not electrically. Furthermore, the magnetic signals obtained often allowed localization of the source, which could be confirmed intraoperatively. These measurements were carried out using single-channel magnetometers and were unable to characterize asynchronous events occurring simultaneously at multiple brain locations. It became clear that progress would be extremely slow until instruments were developed that could simultaneously measure the magnetic field at a large number of sites.

Commercial MEG multi-SQUID systems have evolved from 7- and 37-channel units introduced in the late 1980s and early 1990s to 128-, 122-, and 148-channel helmet systems being produced by companies in Canada, Finland, and the United States. Many of the recent MEG studies have involved an evoked response, in which a characteristic cortical response is stimulated by an external stimulus supplied to the subject. By measuring the magnetic field associated with the response, the functionality of the visual, auditory, and somatosensory areas of the cortex are mapped. Additionally, higher cortical function, such as recognition and attention, may be investigated. Another area of study is spontaneous brain activity, such as the alpha rhythm, during waking and sleeping. MEG is also used in the assessment of sensory pathways between the periphery and the brain, and in the study of stroke, multiple sclerosis, and migraine.

4.2 Magnetocardiography

The first measurement of the magnetic field of the human heart was made in 1963 using room-temperature induction coils of several million turns (Baule and McFee, 1963). Just a few years later, the SQUID sensor became available, enabling a huge improvement in signal-to-noise ratio and stimulating worldwide interest in magnetocardiography (MCG) research. As with MEG, it is felt that combined magnetic and electric measurements are more useful than a single technique alone (Stroink *et al.*, 1992). Clinical applications such as mapping the sources of arrhythmias, ventricular tachycardia, and Wolff-Parkinson-White syndrome may benefit from the development of multichannel instruments. High-resolution SQUIDs have also been used in experimental studies of cardiac tissue slices (Staton *et al.*, 1993), which have contributed to the development of mathematical models of cardiac electrophysiology, and in studies of cortical activity (Okada *et al.*, 1992).

4.3 Other Biomagnetic Studies

SQUID magnetometers have also been used in a number of other biomagnetic applications. By applying a magnetic field to the liver and scanning it with a magnetometer, a susceptibility signal is measured that may be used to estimate the level of stored iron. Unlike the alternative, needle biopsy, this technique is noninvasive and may prove useful in the assessment of hemochromatosis. Magnetic tracers can be used in conjunction with SQUID magnetometers to measure gastrointestinal transit times and in the study of the internal dynamics of cells.

4.4 Geomagnetism

The geomagnetic work done with SQUIDs is primarily divided into paleomagnetism and prospecting. Paleomagnetism is the study of the magnetization of ancient rock for the purpose of understanding the geological history of the region from which the rock was excavated. Prospecting is the search for valuable ore or oil beneath the earth. This may be done by applying a low-frequency electromagnetic field to the earth and measuring the magnetic and electric re-

sponse. By probing at different frequencies, it is possible to determine for the region a profile of the conductivity as a function of depth. This profile is then correlated with geological data to determine the composition of the various strata. Geological mapping of the magnetization of the earth may prove very useful in other ways. In particular changes in the maps over time may be useful in the prediction of earthquakes. Increased stress at the junction of tectonic plates could produce a measurable change in the magnetization of the region.

4.5 Nondestructive Testing

One new field of SQUID research that has attracted considerable interest is nondestructive evaluation (NDE). The NDE SQUID magnetometry efforts of the past decade include flaw characterization, analysis of magnetic properties of materials, and corrosion study. In most of these areas, a measurement of the magnetic field is made at multiple locations in the vicinity of a test object, and a map or image of the field is recorded. Magnetic field sources can be intrinsic in the test object as in the case of galvanic currents flowing in a corroding pipe, or may be excited by an external source. The external field excitation can be done either magnetically or electrically. With magnetic excitation, the test object is placed within a relatively strong magnetic field, whereas a dc or an ac current is established in the sample for electrical excitation using the current injection or current induction method. In the injection method, the metal is directly connected to a current source; for current induction, eddy currents are generated within the inspected region by a coil, wire, or plate carrying an ac current.

The advantages of SQUID NDE are high sensitivity, wide bandwidth (from dc to 10 kHz), and a large dynamic range. The high sensitivity of the SQUID allows one to make engineering and design compromises to reduce cost, enhance signal strength for particular types of flaws, and still remain orders of magnitude more sensitive than other means of magnetic anomaly detection. The ability of SQUID detectors to function down to zero frequency allows them to sense much deeper flaws than traditional eddy-current sensors and to detect and monitor the flow of steady-state corrosion currents. Demonstration experiments have been performed on a wide range of samples, from tracing current in a printed circuit to detecting parasites in fish, but no clear market niche has yet been established.

4.6 Other Applications

It is often said that there are as many SQUID applications as there are SQUID researchers; this is most likely a conservative estimate. This section attempts to show something of the breadth of SQUID research.

There are a number of applications of SQUIDs that do not involve an entire SQUID magnetometer system. A SQUID can be configured to perform as a sensitive picovoltmeter (Clarke, 1966) for a variety of applications, including the measurement of thermoelectric voltages and the study of superconductor mechanisms. The sensitivity of these devices can be on the order of tens of $fV/Hz^{1/2}$. SQUIDs are also used in gravity gradiometers (Paik, 1981) and gravitational-wave detectors (Michelson *et al.*, 1987), where they are configured to sense minute displacements. There has been some development of SQUIDs as radio-frequency amplifiers (Hilbert and Clarke, 1985) and as magnetic resonance detectors (Hilbert *et al.*, 1985). Finally, SQUIDs have been used for a number of fundamental physical measurements, including an investigation into the possible existence of fractional flux quantization (Cabrera *et al.*, 1989), measurement of the Cooper pair mass (Cabrera and Peskin, 1989), and the search for magnetic monopoles (Huber *et al.*, 1990).

GLOSSARY

Bare SQUID: A SQUID operated in the ambient magnetic field, with no magnetic shielding. Typical for the current high-T_c SQUIDs.

Critical Current: The maximum current a superconductor can carry without dissipating energy.

Flicker Noise: Also known as $1/f$ noise. Noise, present in nearly all electrical circuits, with a characteristic rise in amplitude with decreasing frequency.

Fluxoid: The quantum unit of flux, $\Phi_0 = 2.07 \times 10^{-15}$ Wb.

High-T_c Superconductor: Any of a family of ceramic superconductors, discovered in the 1980s, with transition temperatures as high as 133 K.

Magnetocardiography: The study of the magnetic field of the heart.

Magnetoencephalography: The study of the magnetic field of the brain.

Nondestructive Evaluation: The examination of materials or components, without impairing their future usefulness, in order to detect defects and determine serviceability.

SQUID Triangles: The roughly sinusoidal curve of voltage vs applied flux, V_s-Φ_A, of the current-biased bare SQUID.

Tank Circuit: A resonant *L*-*C* circuit.

Tuning the SQUID: Adjusting the bias current I_B to achieve the largest voltage response V_s for a small change in applied flux, $\Delta\Phi \leq \frac{1}{2}\Phi_0$.

Works Cited

Barth, D. S., Sutherling, W., Engel, J., Jr., Beatty, J. (1982), *Science* **218,** 891–894.

Baule, G., McFee, R. (1963), *Am. Heart J.* **66,** 95–96.

Cabrera, B., Cunningham, C. E., Saroff, D. (1989), *Phys. Rev. Lett.* **62,** 2040–2043.

Cabrera, B., Peskin, M. E. (1989), *Phys. Rev. B* **39,** 6425–6430.

Clarke, J. (1966), *Philos. Mag.* **13,** 115–127.

Goodman, W. L., Hesterman, V. W., Rorden, L. H., Goree, W. S. (1973), *Proc. IEEE* **61,** 20–27.

Hilbert, C., Clarke, J. (1985), *J. Low Temp. Phys.* **61,** 263–280.

Hilbert, C., Clarke, J., Sleator, T., Hahn, E. L. (1985), *Appl. Phys. Lett.* **47,** 637–639.

Huber, M. E., Cabrera, B., Taber, M. A., Gardner, R. D. (1990), *Phys. Rev. Lett.* **64,** 835–838.

Jaycox, J. M., Ketchen, M. B. (1981), *IEEE Trans. Magn.* **MAG-17,** 400–403.

Josephson, B. D. (1962), *Phys. Lett.* **1,** 251–253.

Koch, R. H., Rozen, J. R., Sun, J. Z., Gallagher, W. J. (1993), *Appl. Phys. Lett.* **63,** 403–405.

Okada, Y. C., Kyuhou, S., Lähteenmäki, A., Xu, C. (1992), in: M. Hoke, S. N. Erné, Y. C. Okada, G.-L. Romani (Eds.), *Biomagnetism: Clinical Aspects,* New York: Elsevier, pp. 375–383.

Modena, I., Ricci, G. B., Barbanera, S., Leoni, R., Romani, G. L., Carelli, P. (1982), *Electroencephalography and Clinical Neurophysiology* **54,** 622–628.

Paik, H. J. (1981), in: H. Weinstock, W. C. Overton (Eds.), *SQUID Applications to Geophysics,* Tulsa: Society of Exploration Geophysicists, pp. 3–12.

Rifkin, R., Deaver, B. S. (1976), *Phys. Rev. B.* **13,** 3894–3901.

Staton, D. J., Friedman, R. N., Wikswo, J. P., Jr. (1993), *IEEE Trans. Appl. Supercond.* **3,** 1934–1936.

Stroink, G., Lant, J., Elliot, P., Lamothe, R., Gardner, M. (1992), in: M. Hoke, S. N. Erńe, Y. C. Okada, G.-L. Romani (Eds.), *Biomagnetism: Clinical Aspects,* New York: Elsevier, pp. 471–474.

Wikswo, J. P., Jr. (1978), in: B. S. Deaver, Jr., C. M. Salko, J. H. Harris, S. A. Wolf (Eds.), *Future Trends in Superconductive Electronics,* AIP Conference Proceedings No. 44, pp. 145–149.

Wikswo, J. P., Jr., van Egeraat, J., Ma, Y. P., Sepulvada, N., Staton, D. J., Tan, S., Wijesinghe, R. S. (1990), in: A. F. Gmitro, P. S. Idell, I. J. LaHaie (Eds.), *Digital Image Synthesis and Inverse Optics,* SPIE Proceedings No. 1351, Bellingham, WA: SPIE, pp. 438–470.

Zimmerman, J. E., Silver, A. H. (1966), *Phys. Rev.* **141,** 367–375.

Further Reading

General

Clarke, J. (1989), in: H. Weinstock, M. Nisenoff (Eds.), *Superconducting Electronics,* Berlin: Springer-Verlag, pp. 87–148.

Simon, R., Smith, A. (1988), *Superconductors: Conquering Technology's New Frontier,* New York: Plenum Press.

Tinkham, M. (1975), *Introduction to Superconductivity,* New York: McGraw-Hill.

Applications

Donaldson, G. B. (1989), in: H. Weinstock, M. Nisenoff (Eds.), *Superconducting Electronics,* Berlin: Springer-Verlag, pp. 175–207.

Fagaly, R. L. (1990), in: S. Sato (Ed.), *Advances in Neurology* Vol. 54, New York: Raven Press, pp. 11–32.

Swithenby, S. J. (1980), *J. Phys. E: Sci. Instrum.* 801–813.

Wikswo, J. P., Jr. (1995), *IEEE Trans. Appl. Supercond.* **5,** 74–120.